1. DELIVERABLE REPORT

2. FRONT PAGE

DELIVERABLE REPORT

Grant Agreement number: 248835

Project acronym: SPEDOC

Project title: Surface Plasmon Early Detection & Treatment Follow-up of Circulating Heat Shock Proteins & Tumor Cells

Funding Scheme: FP7

Deliverable reported: D2.5, ODP demonstrator and conclusions, High throughput microfluidic device

Due date: M42

Name, title and organisation of the scientific representative of the project's coordinator: Dr. Romain Quidant, ICREA Professor, Plasmon nano-optics group. ICFO-The Institute of Photonic Sciences

Tel: +34 93 553 4076

Fax: +34 93 553 4000

E-mail: romain.quindant@icfo.es

Project website address: www.spedoc.eu

Name, title and organisation of the scientific representative of the Deliverable reporter:
Rafael Porcar, Business Manager, COSINGO Imagine Optic Spain SL

Date: 23 / 08 / 2013

Signature of reporter and scientific representative of the Coordinator:

3. Objective

The objective of WP2 is the design and production of a prototype of an optical detection platform (ODP) for early cancer detection. For the reported task T2.5, objectives where, as described in Annex I are:

- Production of the ODP demonstrator
- Development of a high throughput device platform for highly parallel analyte detection.

Index of the delivery report:

3. Objective 3

4. Progress towards objectives 3

5. Deviations 4

6. Detailed explanations 4

2.1 ODP: Man Machine Interface coding 4

2.2 ODP: Production and assembly the new Optical Detection Platform version 8

2.3 ODP: Test of the new Optical Detection Platform version 10

7. Annex 16

2.4 Design and functional analysis of the new ODP 16

4. Progress towards objectives

- Production of the ODP demonstrator [COSINGO]: To go a step further toward the commercialization of the Optical Detection Platform, the task "T2.5. production of the ODP" included in the reporting period an important upgrade of the control software COSINGO developed, called *Biofractix*. When the first version was simply intended to control the instrument and allow us to validate the functions we were implementing, this new upgrade had been designed to optimize workflow for the user, making each step more intuitive and avoiding possible error in the procedures that could lead to wrong data acquisition. Less difficult to see from the interface, but even more important, the code structure had been optimized to gain in robustness, including internal error management, optimizing computing time, etc.
  In the last stage of the project (from M37 to M42) we have taken advantage of the project extension to mount, debug and test the new device successfully.

- Development of a high throughput device platform [EPFL, Maerkl's group]: We developed a multiplexed high-throughput nanoimmunoassay chip capable of quantifying four biomarkers in 384 5-nL biological samples for a total of 1,536 assays. Our sample throughput is 30 times higher than recent integrated microfluidic devices (Heath et al, Nat Biotech, 2008, and Huang et al, Lab Chip, 2012), with an order of magnitude higher assay throughput. This ultra high-throughput translates into a 1,000 fold reduction in reagent costs. The limit of detection is 100 fM, a similar performance as ELISA, but is achieved by detecting as few as 600 antigen

molecules in 5-nL samples (~1 zeptomole), which is 20-fold lower than current state-of-the-art techniques (Duffy et al, Nat Biotech, 2010). The chip is compatible with a number of complex biological matrices including blood serum, cell culture medium, and bronchoalveolar lavage (BAL).

5. Deviations

The delivery date of this report corresponding to D2.5 has been moved from M36 to M42 due to the project extension. We report then our developments from M25 to M42. Again, the project extension asked by reviewers of the project was the opportunity to complete successfully with the objectives of the WP2, T2.5.

Although the design part of the new ODP corresponds to Task 2.4, and should be in Deliverable D2.4, as this task has be closed and corresponding deliverable submitted on time on month M27, we place in annex the work performed on task 2.4 during the extension period from M36 to M42.

6. Detailed explanations

2.1 ODP: Man Machine Interface coding

To target efficiently our audience, it was necessary to develop a user interface to control our Optical Detection Platform that allows:

- a complete control of the acquisition and calibration of the device,
- a good ergonomy that make easy and safe this control and let users focus on the biology part of the experiment,
- an open access to data acquired for post processing in the environment wanted by users.

We present in this section the new version of Biofractix, the control software of the Optical Detection Platform. It contains new features, new ergonomics properties of the interface (workflow had been totally redesigned to make steps toward data acquisition fewer and more intuitive) and it is based on an optimized code (the number and justification of the states of the finite state machine, inherited of two years of tests and improvements, had been cleaned, intensive bug test had been performed by non-expert users, internal time sequences had been measured and optimized).

New features:

- Centroid graph window: sensorgrams display.

Biofractix application allows select up to 16 different positions of measurement in the sensing chip area. This new window presents the results, in real time, of the experiments with the possibility for the user to select which sensorgram(s) to display.

- HTML button: automatic report generation gives to the user the option to save the measurements done (the sensorgram(s) but also main acquisition parameters) in a HTML file. This file is opened in the Explorer and saved in the same path than the data file.
- Help button: online help.

opens “User Documentation Biofractix.pdf”. This document is meant to explain, to an un-experienced user, how to use the software for LSPR sensing experiments. All the features from acquisition configuration to data plotting and exportation are detailed and commented with screenshots.

- Microfluidics window: control the on chip valves.

In this upgrade, we have introduced the option to control different version of sensing chips. user can also actuate individually on all electronic valves (up to 32 valves maximum).

New interface:

We go through the main windows of the new software hereafter:

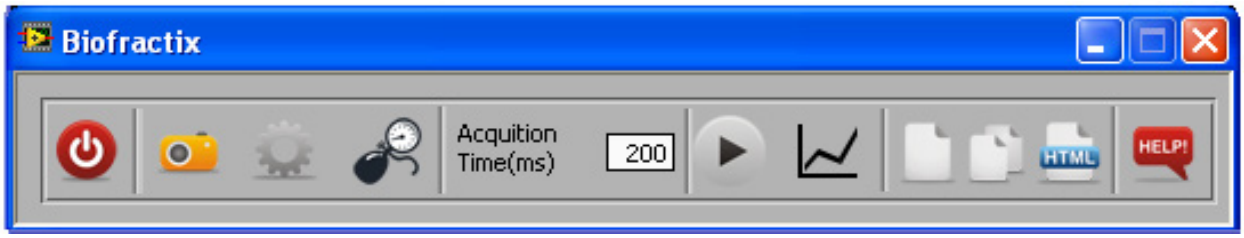

Biofractix interface: principal control panel

The screenshot below shows the main panel of Biofractix interface software. From it, user can perform any action on the ODP. It contains three different functional areas dedicated to (from left to right):

1. Measurement configuration,
2. Data acquisition,
3. Data management.

We go through the secondary windows of the new software hereafter:

Button	Action	Windows
	Opens a secondary window that allows:	**Camera window**
	Visualization of the chip, its valve, nanostructures at the ROI, etc.: User can: - adjust Exposure Time of CCD - calibrate Cursor position where the sensing is performed	
	Opens a secondary window that allows:	**Extinction window**
	- Configuration of single measurement.	

	- Allows adjust the ROI position. - Displays RAW spectrum (resonance or reference) and extinction for the actual ROI.	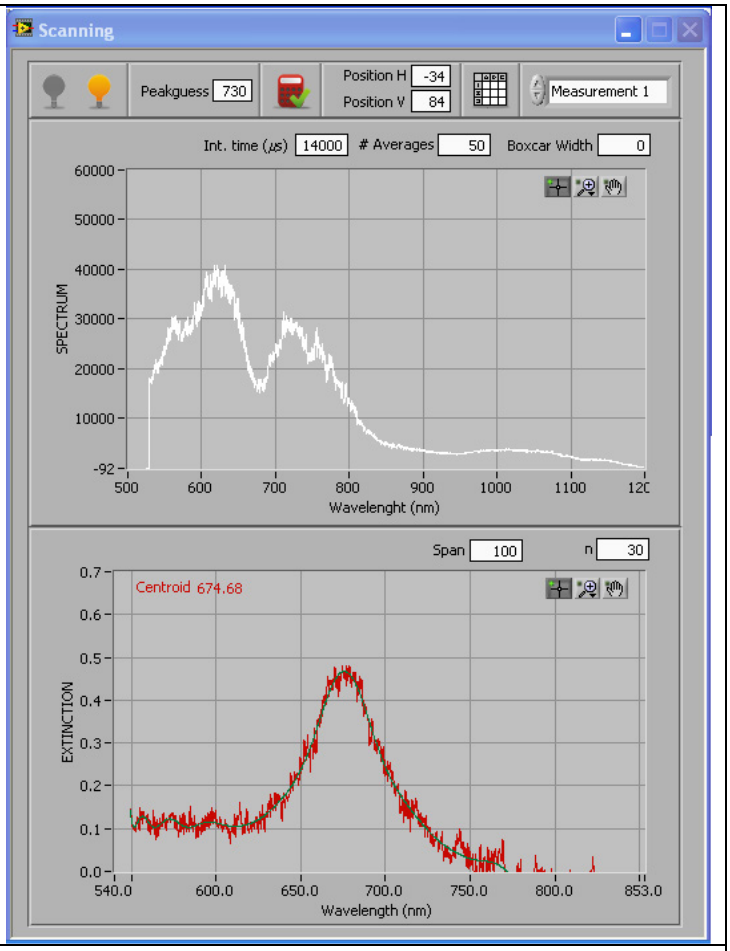
	Opens a secondary windows that allows:	**Table configuration window**
	- to choose and save all the ROIs that will be scanned in multiplexed measurement, and their corresponding references: their position as well as complementary parameters.	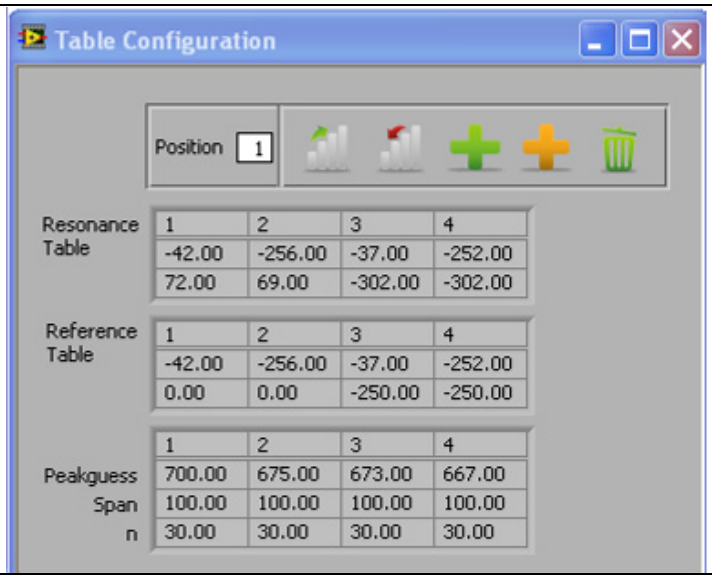
	Opens a secondary window that allows:	**Microfluidics window**

	- 4 chambers chip selected. - Configure flow protocols to control valves in a multiplexed way (user customized). - Optional individually control of the valves	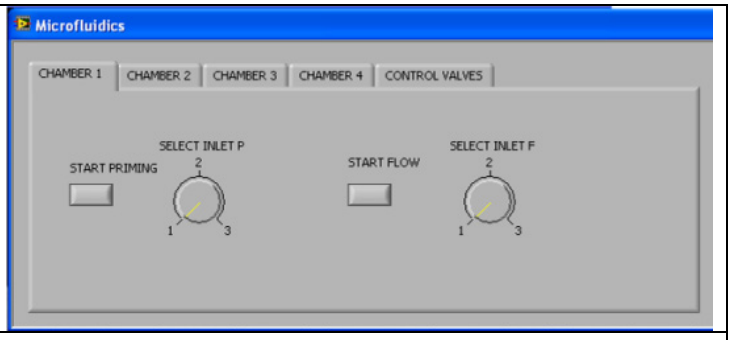
	Opens a secondary window that allows:	**Sensorgram windows**
	- Allows monitoring up to 8 ROIs in real time. - Individual selection of sensorgram up to 8. - Statistic for each ROI: mean value, STD (noise), Slope of the curve (stability).	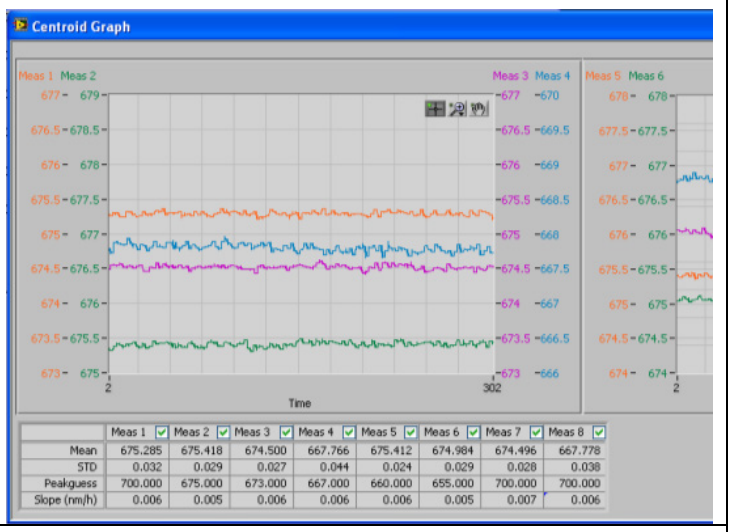
	Opens a secondary window that allows:	**Export data**
	- ASCII tabulated file for post-processing - File contains extinction position only.	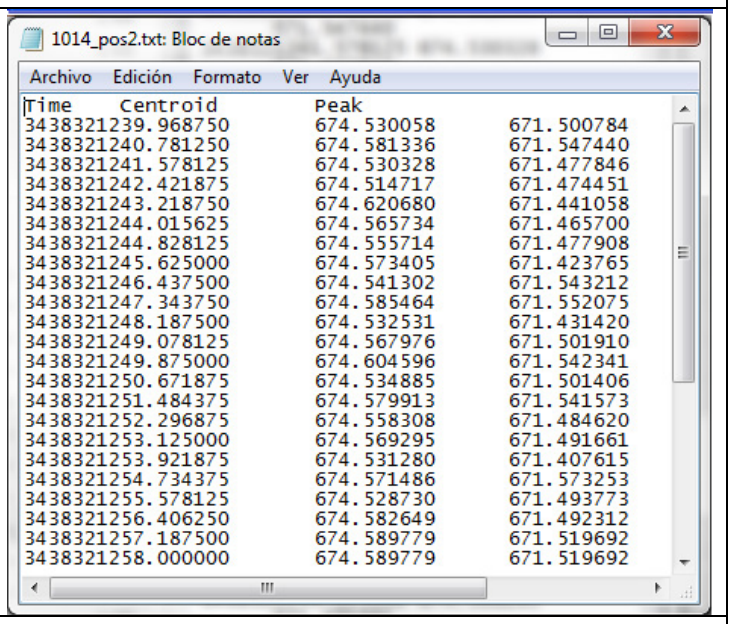
	Opens a secondary window that allows:	**Advanced export data**

<table>
<tr><td></td><td>- ASCII tabulated file for post-processing
- File contains all the RAW intermediate spectrum and complementary acquisition parameters for full post processing and debugging.</td><td> 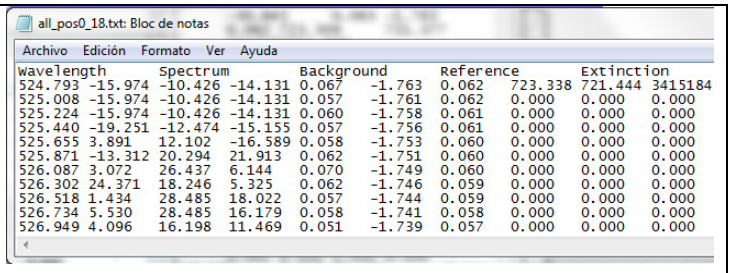
</td></tr>
<tr><td>  </td><td>Opens a secondary window that allows:</td><td>Automatic report</td></tr>
<tr><td></td><td>- generate an html file for easy visualization of data even once Biofractix is closed.</td><td> 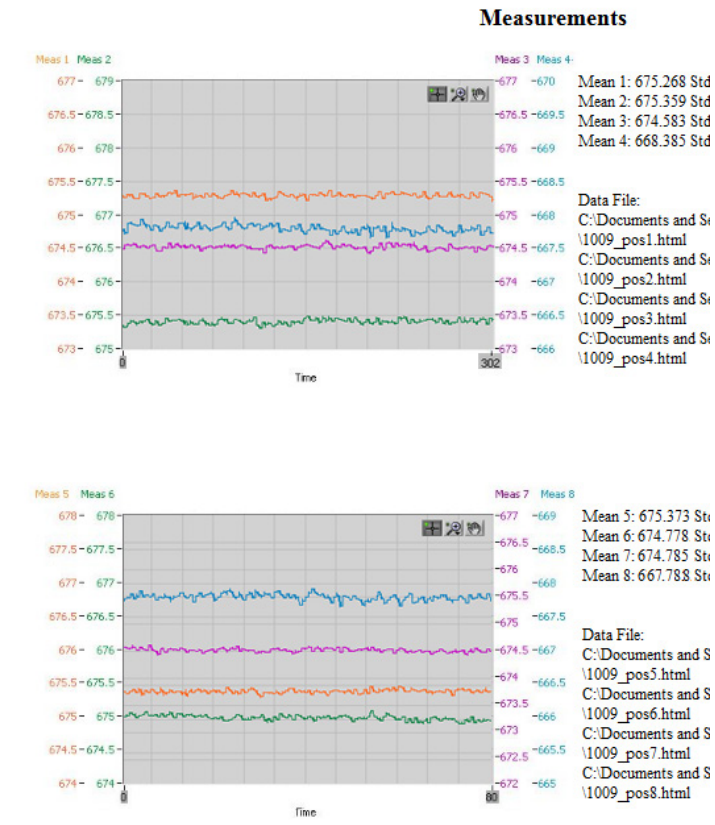
</td></tr>
</table>

Secondary windows and reports of Biofractix interface software

2.2 ODP: Production and assembly the new Optical Detection Platform version

Once complete optical, electronical, mechanical design finalized, we started the production process of the ODP within the extension period (M37 to M42) in order to get it finalized on time before the end of the project.

Below are the mechanical parts that constitute the heart of the platform: the sensing module, and hold the optics and allow for its adjustment.
the coating we apply to aluminium protect it from aging and to reduce possible reflections of light on the metal.

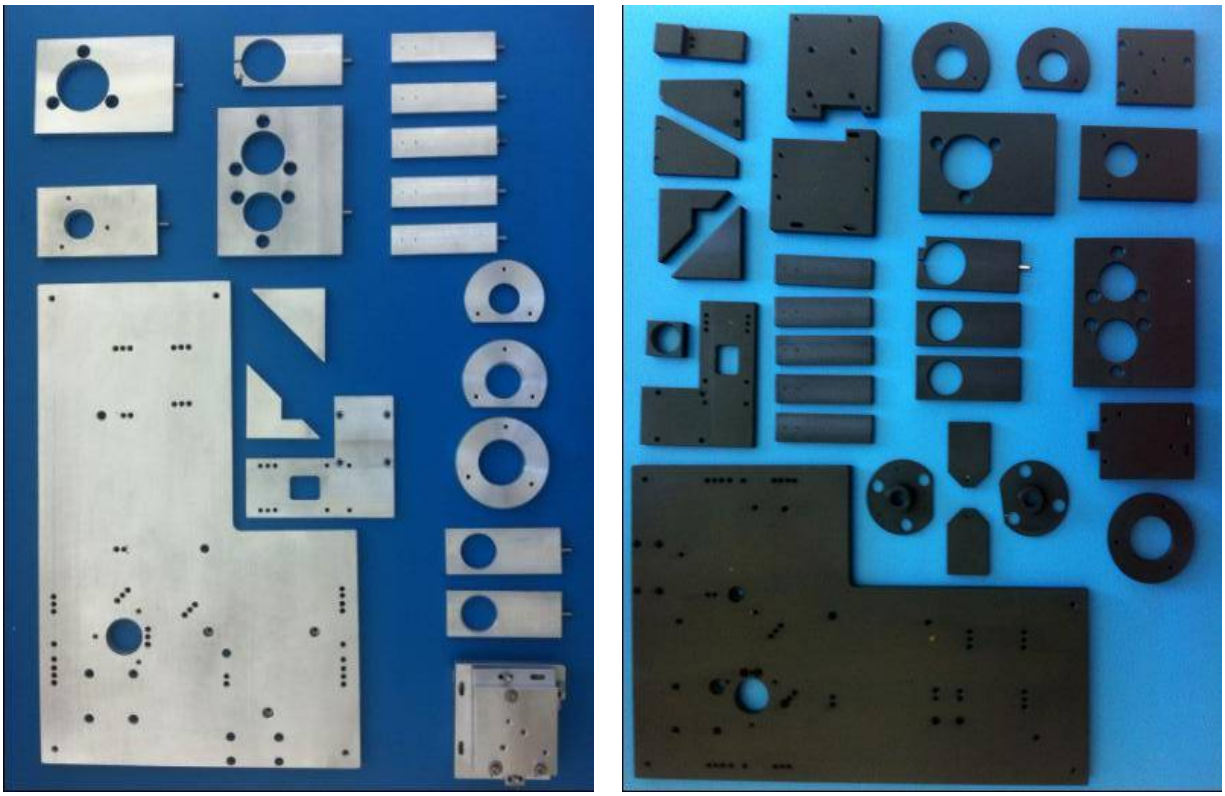

Pictures of the RAW mechanical parts before anodizing (left), and after (right)

We then proceed to the assembly of the complete device to validate the new design. Hereafter are the three modules constituting the ODP demonstrator.

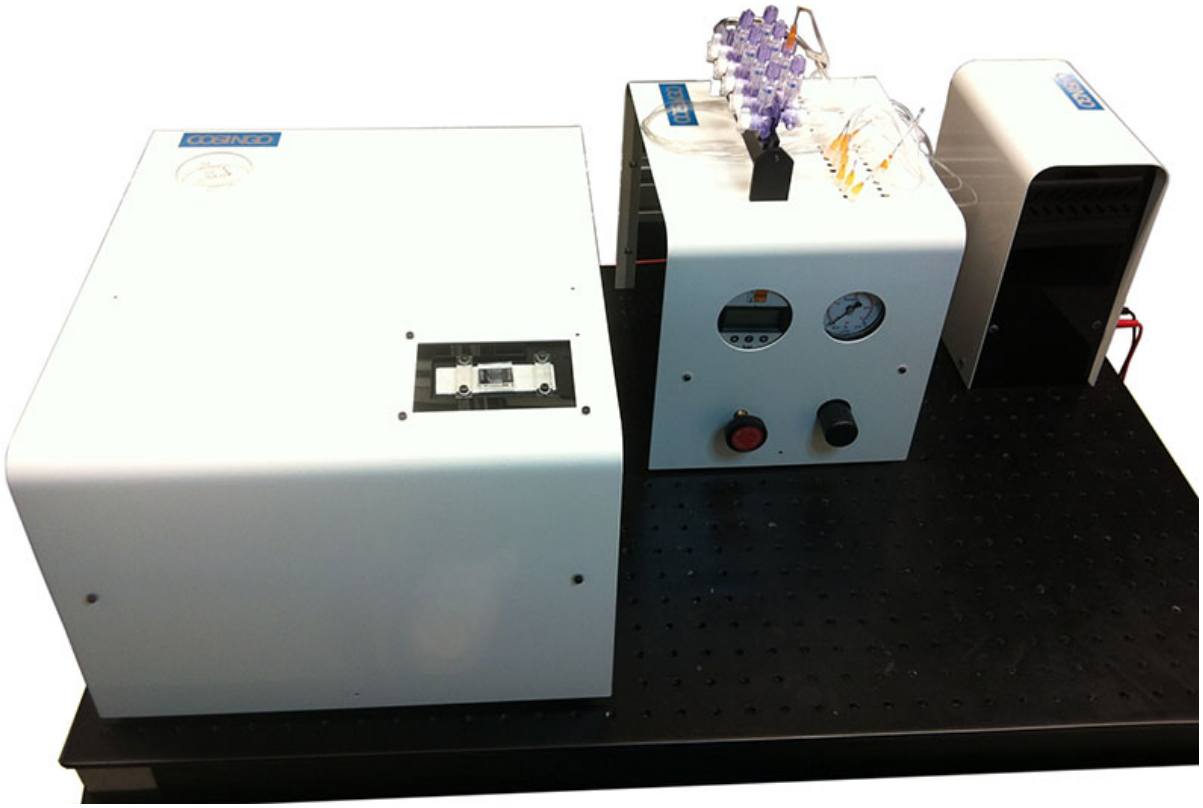

From left to right: sensor, microfluidic and illumination modules

2.3 ODP: Test of the new Optical Detection Platform version

We validated the new ODP repeating standard tests applied on previous version of the ODP. The first experiments with the new detection platform have been addressed to analyze its stability. In these experiments, we measured the resonances of an array of gold nanorods on PDMS substrate, provided by partner 1 (ICFO).

Noise:

In the following figure, the centroid position for the sample measured over 10 minutes is plotted. The standard deviation of the centroid is 0.008 nm rms. The level of noise is equivalent to the noise observed with the first prototype and no drift is observed over 10 minutes.

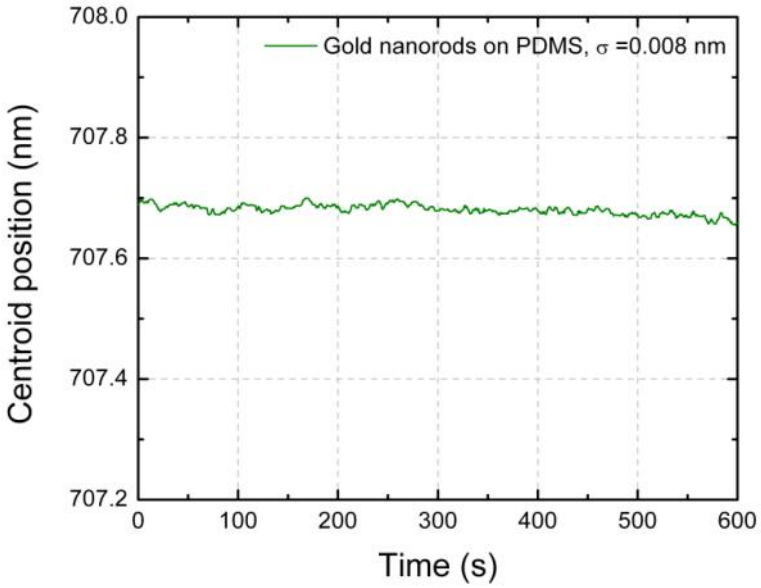

Centroid position of the resonance of gold nanorods on PDMS substrate measured with the new ODP platform.

Conclusion: noise for short time (which can be assimilated to resolution) is excellent, and as good as previous version. Noise for largest period of time (stability of the device) is better than previsou ODP version. Noise: 8pm rms.

Noise under multiplexing conditions:

The same experiment was performed using the multiplexing capabilities of our instrument, measuring in two different positions of the sample. In this kind of experience, the system sequentially acquires the reference and resonance signals and for each position, scanning then 4 ROIs in 2 different chambers. The Figure W.P 2.17 resumes the results.

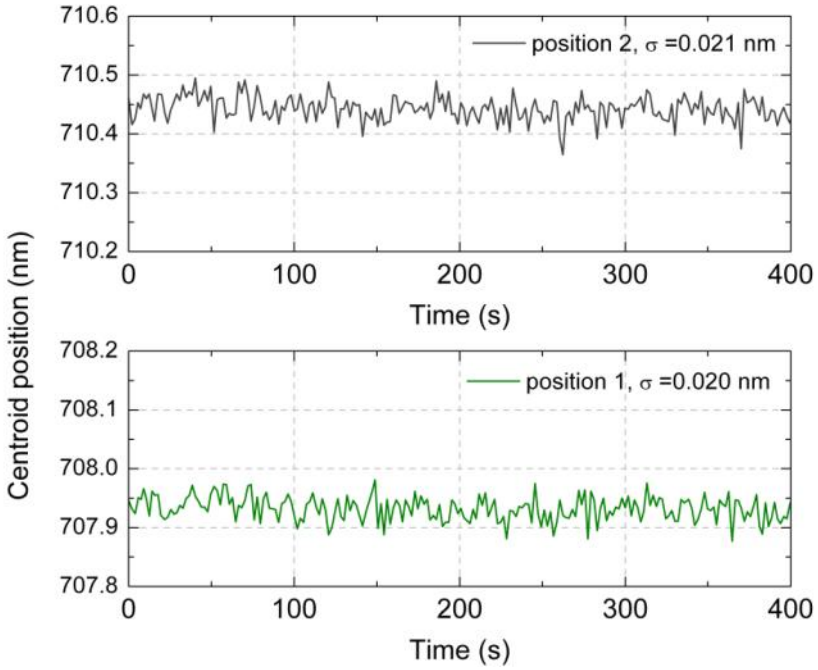

Centroid position of the resonance of gold nanorods on PDMS substrate measured for two different positions.

As we can see, the noise level is significantly higher than that obtained by measuring in one position (when the signal is not updated dynamically reference). Similarly, despite of this, resulting noise level is comparable to that obtained with the laboratory equipment. Also, as in the previous experiment, the centroid position curve does not exhibit drifts.

Conclusion: The stability and noise of our optical detection platform is comparable to the state of the art laboratory systems. We can appreciate that the measurement based on mobile parts such as the galvo that performs the multiplexing function, present more noise: 20pm rms.

Sensitivity of the device:

As additional testing of the device, we repeated bulk refractive index measurement, in the same way that it had been performed up to now

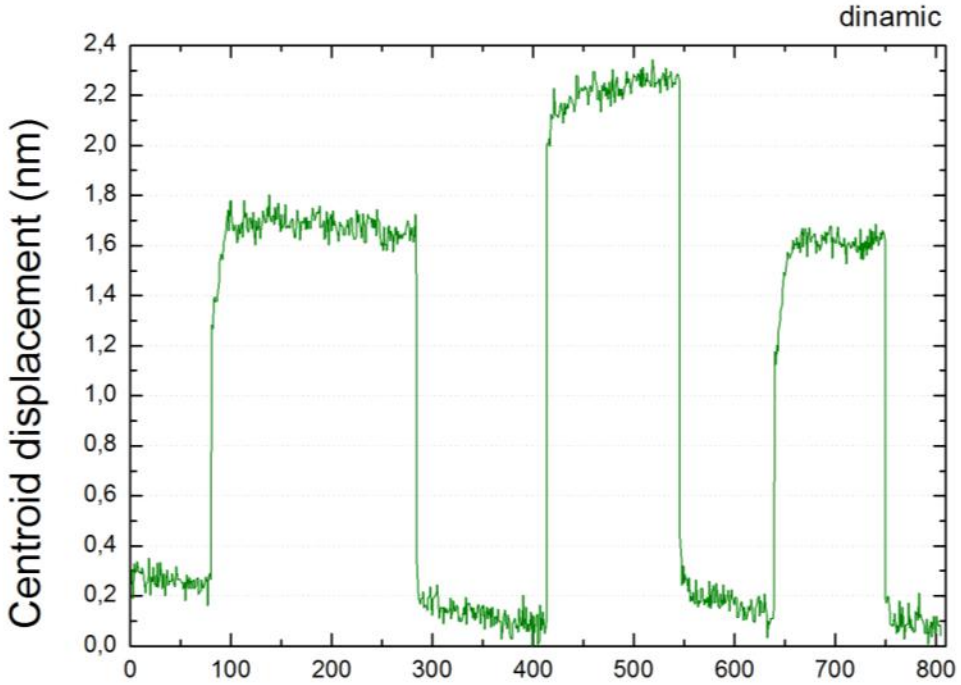

Displacement of the extinction, during a refractive index experiment

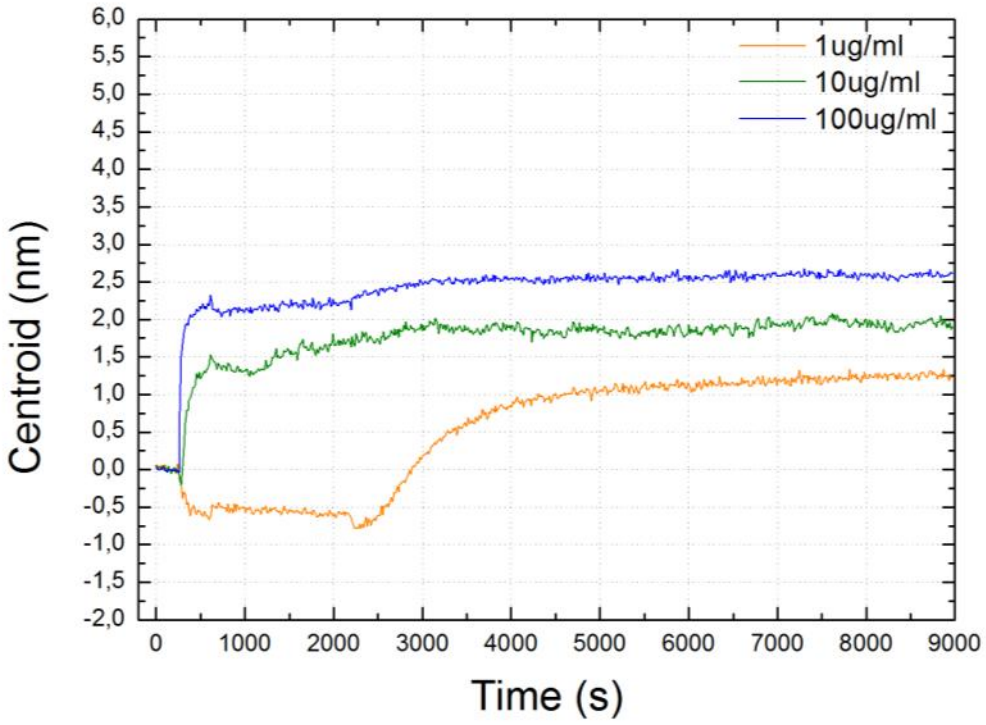

streptavidin calibration curve, Displacement of the extinction for several concentrations

Conclusion: The sensitivity is the same than previously, which is not surprising as it mainly rely on the chip and not on the platform. The new design does not affect this parameter. Calibration curves are good. We did not reach the minimum detection of the antibody, as for

the smallest concentration, we still detect a large shift of the resonance. We'll then repeat the experiment with lower antigen concentrations.

High throughput micro**fluidic chip**

We applied the platform to the large-scale analysis of the cytokine response of dendritic cells (DCs) to a large number of binary adjuvant combinations. Finding novel, and potent adjuvants and adjuvant cocktails is of paramount importance for the design and development of novel therapeutic vaccines. We applied our nanoimmunoassay chip to measure the cytokine response of DCs in the largest adjuvant screen conducted to-date. We measured 435 combinations of 10 different adjuvants and quantitated extracellular levels of 4 cytokines in each sample. Our nanoimmunoassay chip enabled the large-scale screening of adjuvants by reducing reagent cost from ~20,000 Euros down to 15 Euros, and by automating and streamlining the entire process. We discovered new adjuvant combinations that could be used in the production of vaccines. We quantified cytokine levels in mouse serum and BAL for two of the newly discovered adjuvant cocktails, which confirmed the synergistic effect in vivo.

Aside from applications in systems immunology and systems biology, our nanoimmunoassay chip will have significant impact on the healthcare sector by drastically reducing the cost of diagnostic assays. In fact, in the near future it will be possible to routinely and periodically screen small blood samples from healthy individuals for large panels of disease indicators. With technologies like the nanoimmunoassay chip described here, the cost of such preventative screens will be minimal, and be far outweighed by the benefits and cost reductions associated with early diagnosis of disease

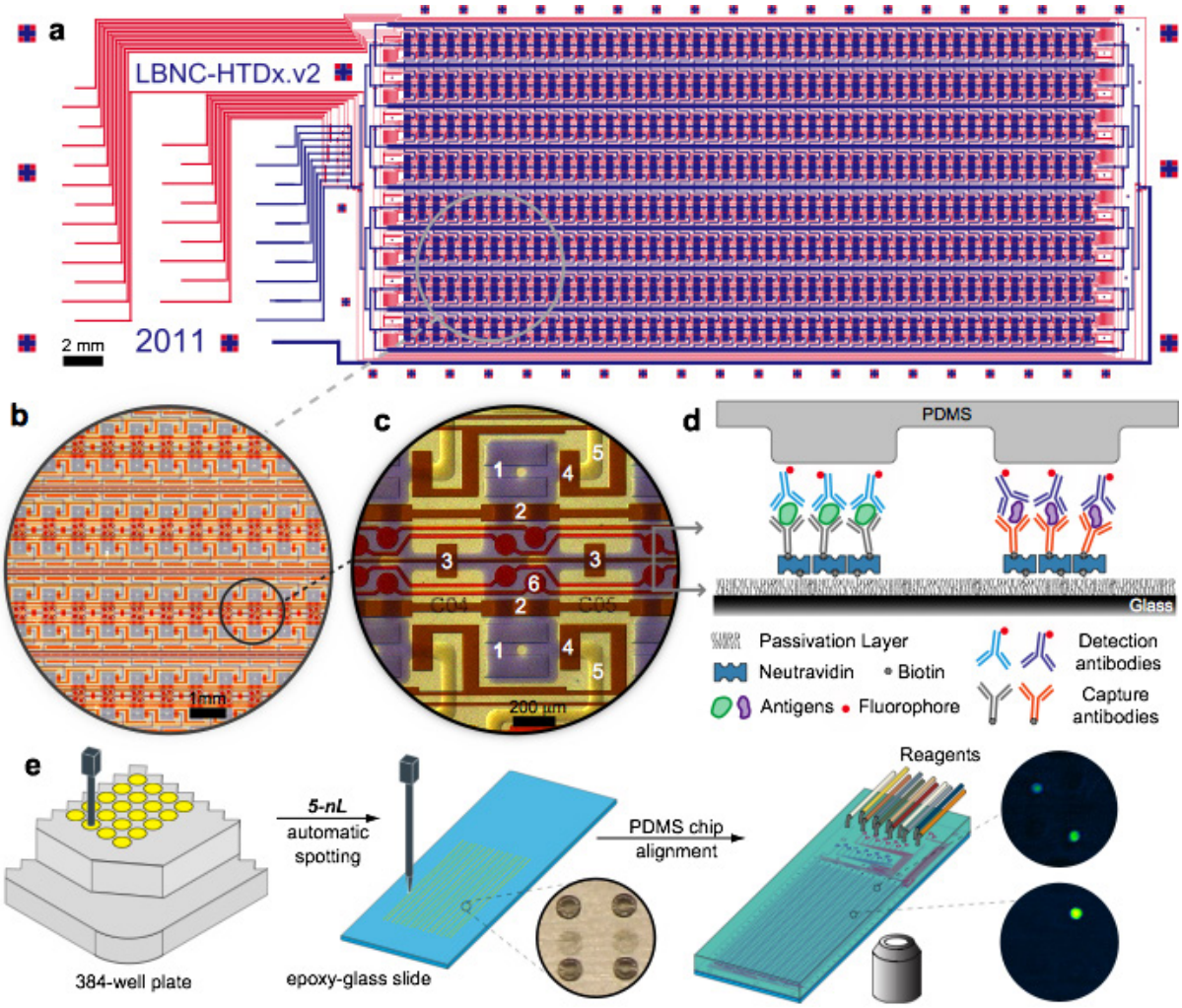

Figure WP2.14: Nanoimmunoassay chip workflow. (a,b) The microfluidic device (a) consists of flow (blue) and control (red) layers, divided into eight rows (b), each row containing 48 single assay units for a total of 384 units. (c) Each assay unit contains two spotting chambers (1) and an assay chamber in the middle. Chamber valves (2) separate the spotting chambers from the assay chamber during surface derivatization. Assay units are isolated from one another during incubation by isolation valves (3). Relief valves (4) help release built-up pressure into a microfluidic channel (5) after incubation. Four "buttons" in the assay chamber define and protect the circular immunoassay regions (6). (d) A sandwich immunoassay is performed under each "button" valve with a combination of biotinylated and fluorophore-labeled antibodies. (e) Biological solutions in microtiter well-plates are automatically spotted onto an epoxy-coated glass slide using a microarray robot. Dried spots have a diameter of ~350 µm. A microfluidic chip made by multilayer soft-lithography is aligned on top of the spotted slide. Surface chemistry is generated and biomarkers are detected with a fluorescent scanner.

Surface micropatterning of proteins is central to a large number of approaches in cell biology, tissue engineering, and integrated diagnostics. We developed a microfluidic approach for the multiplexed patterning of several proteins integrated within a single assay unit. By pressure modulation of a simple fluidic button-membrane we were able to form several concentric annuli, each consisting of a specific protein. We further showed that the external control pressure can precisely tune the size of each annulus, and the entire approach can easily be scaled to thousands of assay units. To show the potential of our approach in the context of integrated diagnostics we applied the method to a multiplexed immunoassay. The approach

developed thus has the potential to increase throughput of molecular measurements conducted on current microfluidic devices by over an order of magnitude.

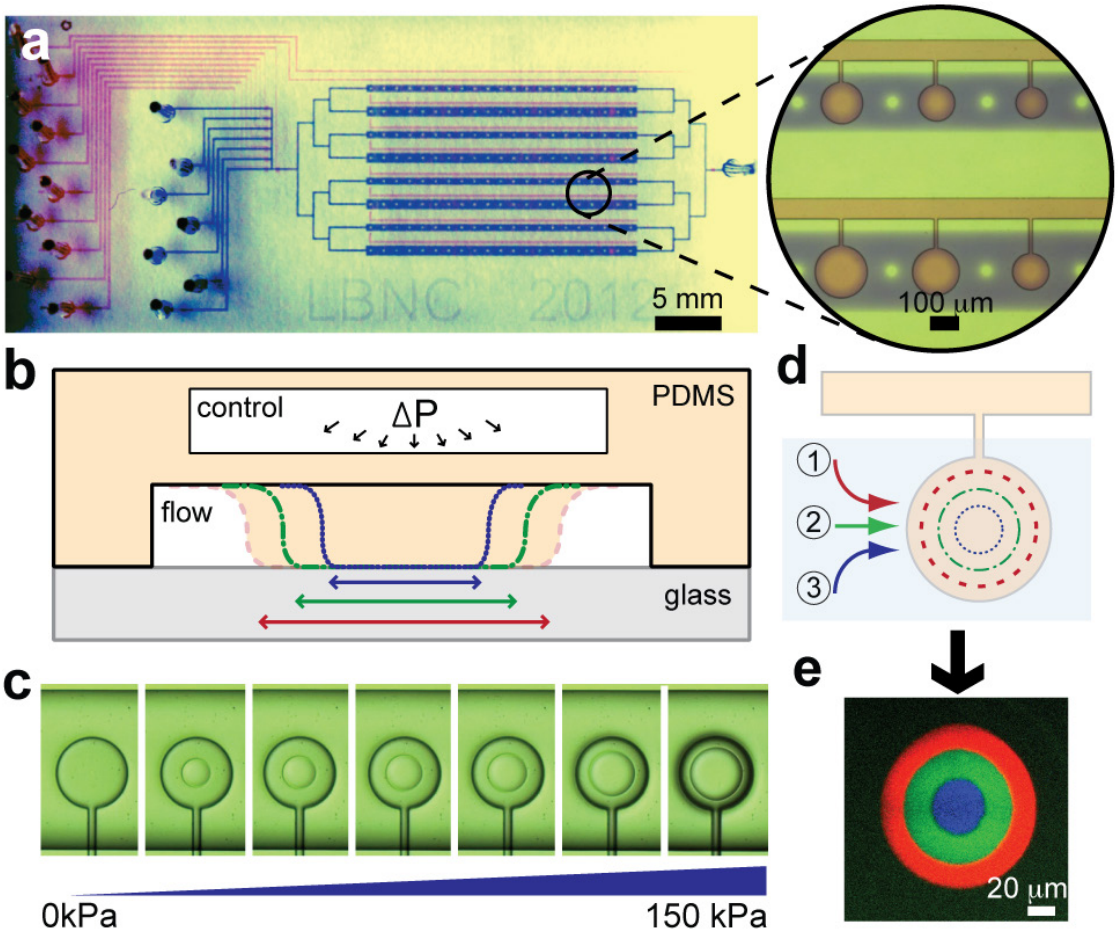

Figure WP2.15: Protein patterning with a microfluidic button-membrane. (a) Photograph of the device. Inset shows button-membranes (red) aligned to flow channels (blue). (b) Schematic cross-section of a button-membrane and flow channel. The PDMS membrane is deflected downwards with increasing pressure. (c) A series of photographs show the area in contact with the substrate at various pressures (0 - 150 kPa). (d) Multiple proteins can be immobilized in the form of concentric annuli. The first protein is introduced into the chip with the valve actuated at the highest pressure, followed by a washing step. The pressure is decreased slightly and the next protein introduced. These steps are repeated successively for the rest of the proteins. (e) Fluorescence image of three different types of fluorescently-labeled neutravidin patterned using this approach.

7. Annex

2.4 Design and functional analysis of the new ODP

In the last stage of the project (from M37 to M42) we have taken advantage from the knowledge generated during the development and the functional analysis of the first optical detection platform, for redesigning a new version of the device. As we will see, the new platform presents better ergonomics for users over the previous version from a commercial standpoint over the previous version.

The new instrument consists of three separate modules: the microfluidics module, the sensor module and the illumination module.
This new breakdown of the ODP into modules offers a number of advantages from the point of view of the platform assembly (allowing, for example, the extraction of the optical part as a whole for its optical alignment during production), support (making easy the update of its components) and modularity (allows the end user to integrate their components (eg light source) on our platform, or to choose between several microfluidic control devices, etc.)
This new implementation clearly corresponds to exploitation requirements and represents a step toward a commercial product.

The new ODP includes the following general improvements:

- The sample is placed in horizontally in order to provide more stability. The new orientation of the sample facilitates its manipulation during the filling of the microfluidic channels.
- The plasmonic resonances are acquired in a reflection configuration. The reflection-based measurements allow for a more compact and simple optical setup and let the microfluidic chip free of access to end-user.
- We have added the scanning function on the CCD camera, improved its resolution and image quality within the FOV.
- The optical system halved the number of lenses of the detection platform. The reduction of optical elements is performed maintaining optical quality while decreasing costs of the system.

Optical design:
The new optical system presents the following characteristics:

- The detection is based in a reflection configuration.
- We have added the scanning function on the CCD camera by placing it after the galvanometric mirror. With the new position, the field of view of the CCD can be displaced with the rotation of the galvanometric mirrors and the measurement area is always located at the same point of the field of view.
- The optical system halved the number of lenses of the detection platform. The reduction of optical elements minimizes the optical aberrations.

Features	Prototype (device v1)	Demonstrator (device v2)
Illumination		
Illumination beam	Adjustable from collimated to focused	Focused
NA	0.13	0.18

Wavelength	Broad spectrum (Tungsten lamp) 500 – 850 nm	
Detection		
Detection diameter (ROI)	50 µm	50 µm
Spectral range	550-1050 nm	567-1050 nm
Scanning		
FOV (on chip)	10 x 10 mm	2.5 x 2.5 mm
Visualization, CCD		
FOV (on chip)	6.26 x 4.76 mm	3.13 x 2.38 mm
Scanning	No	Yes

The Table resumes de characteristics of both optical systems.

Zemax simulations:

The optical design of the new platform has been based on an optical simulation using Zemax, which is a widely-used program for the design and analysis of optical systems. Zemax includes a vast library of commercial elements (different manufacturers) that allows us to realistically simulate the response of an optical system. In addition, we have simulated the optical paths of the previous version of the ODP in order to compare the properties and the optical aberrations between both systems.

The analysis has been done by setting an object of 50 um diameter, which represents a circular area located on the nanostructure. Then, we have determined the spot diagram of the image plane of the system, e.g, in our case, at the plane where is located the fiber of the spectrometer.

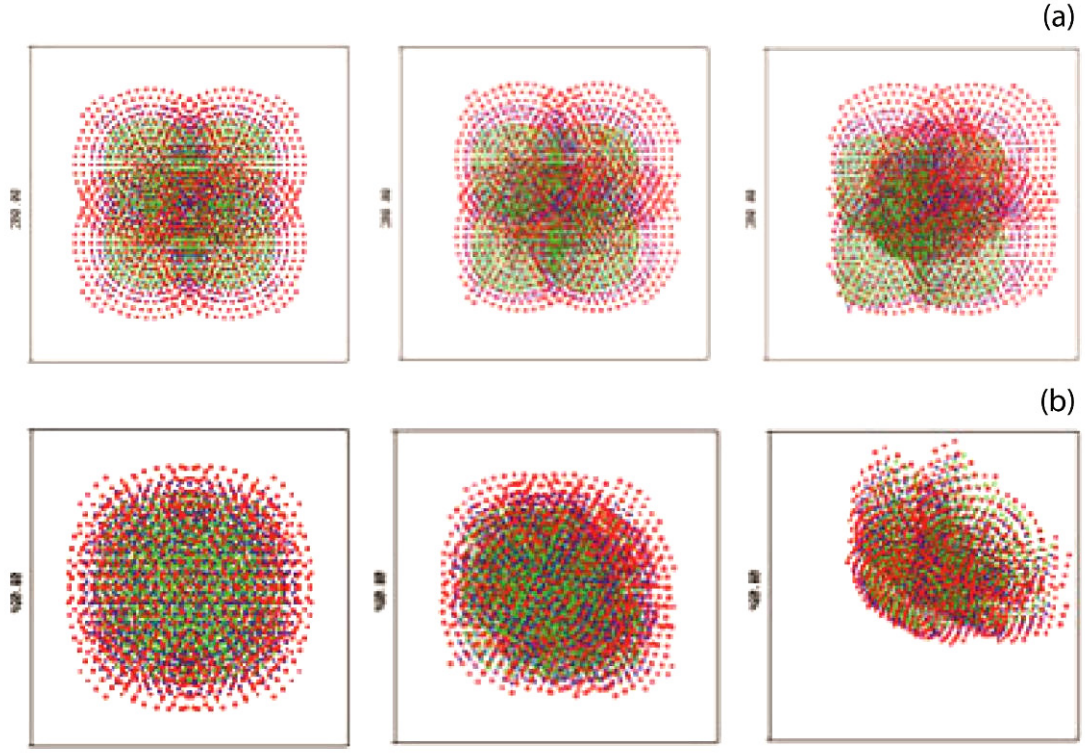

Figure WP.2.15: Spot radius at the detection plane of a circular area of 50 nm diameter, for the new (a) and old (b) optical systems. The box sizes 200 nm (a) and 400 nm (b) respectively.

Figure WP.2.15 resumes one result of these simulations. The figure shows the spot radius at the image plane for different displacements of the measurement area. We have measured the

spot radius for displacements of: 0, 1.3 and 2.6 mm. The displacement is produced by the rotation of the mirrors.

As we can appreciate, for the same movement, the image point obtained with the simulation of the new system better maintains its sphericity. This indicates that the optical aberrations of the latter are lower. Furthermore, although the magnification is similar for both optical systems, the image size differs significantly.

-> *Conclusion 1*: The simplification and optimization of the optical system has resulted in a decrease of the optical aberrations. Thus, the new optical system, based on the measurement of the reflected light, present better performance than the previous one.

Mechanical design:

a. Optical Sensor (within sensor module).

A new mechanical implementation has been designed to integrate the new optical design presented previsously, based for this version on fully custom mechanical parts. The use of custom parts brings a complete freedom to design the compact implementation. So we designed the optical sensor support considering the following objectives:

- Create mechanical adjustments that allow an easy alignment of the optical path. Simplify adjustement of the position of the optics respect with classical pieces to make it faster and cheaper to produce.
- Create the simplest holders, with only the necessary degrees of freedom, in order to make the prototype more compact robust, which means fewer risks of misalignment during shipment and use of the ODP.
- reduce the costs of the parts (if we don't consider time spent to design it) even producing only one unit of the platform, respect with the implementation made with off the shelf part from manufacturers like Thorlabs.

The result of the mechanical design is presented in the next picture:

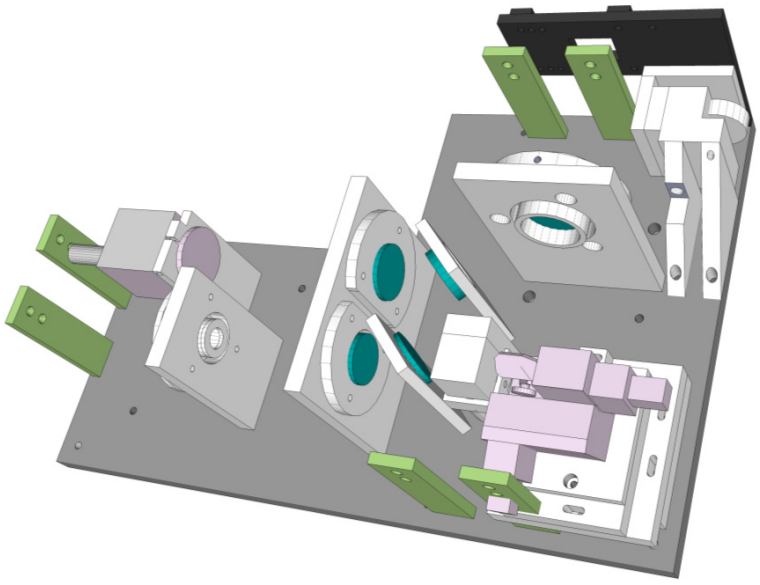

3D CAD design Optical Sensor.

It is made of more than forty mechanical parts (light grey) allowing either transverse adjustements, along axis translation for correct focusing, angular orientation, etc. They are all

mounted on top of a common base plate (dark grey) for robustness. Optical components (blue) are glued to simplify the assembly. Alignment tools (green) have been foreseen to simplify production fo the sensor.

Last step of the design is to generate the layouts of each part, for the mechanical workshop, as presented in the next image.

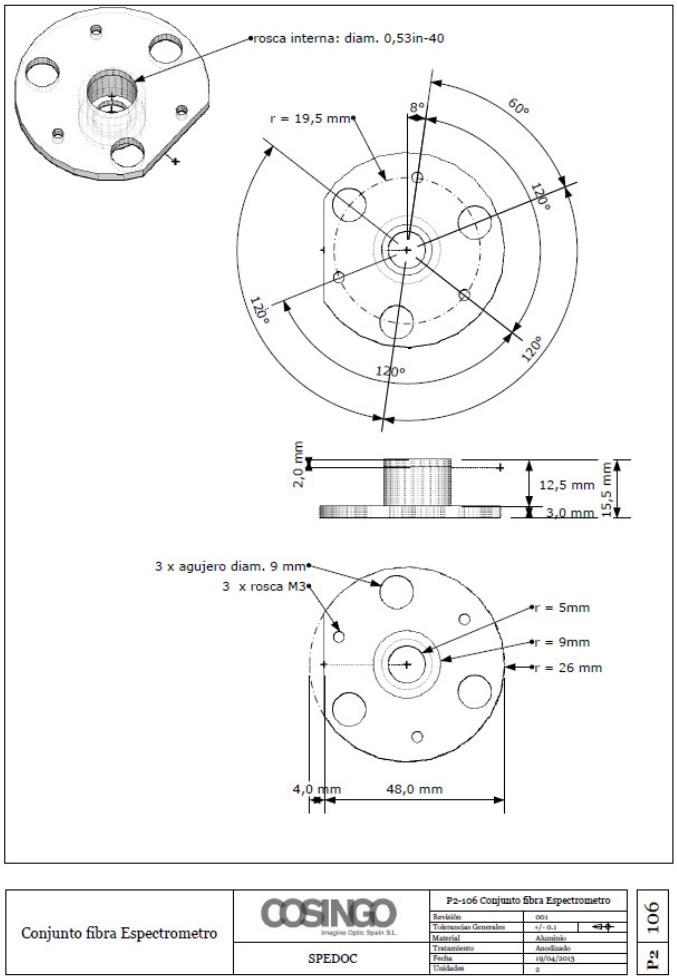

Example of mechanical layout.

b. Complete prototype.

As introduced in the general features part, we have divided the machine in three functional modules:

- Illumination
- Microfluidics
- Sensor (and electronic control),

which we present in detail in the following paragraphs. Structure of the module has been based on rails assembly for its modularity. Module frames are made of metal sheeting, bent and painted for good finished quality.

- Illumination module:

The illumination is important to separate from the rest of the optical sensor because it generates a significant power dissipation which results in temperature rise, and therefore might interfere with the measurement stability.

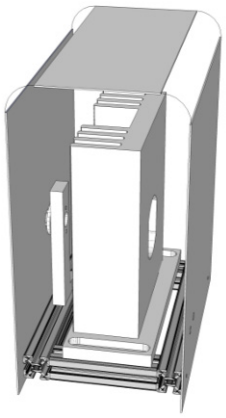

3D CAD of the Illumination module.

- Microfluidics module:

In this version we have increased the number of solenoid valves (from 24 to 36) in order to allow the control of more complexe chips.The tilting mount of the manual valves, allows an easier access for the user.

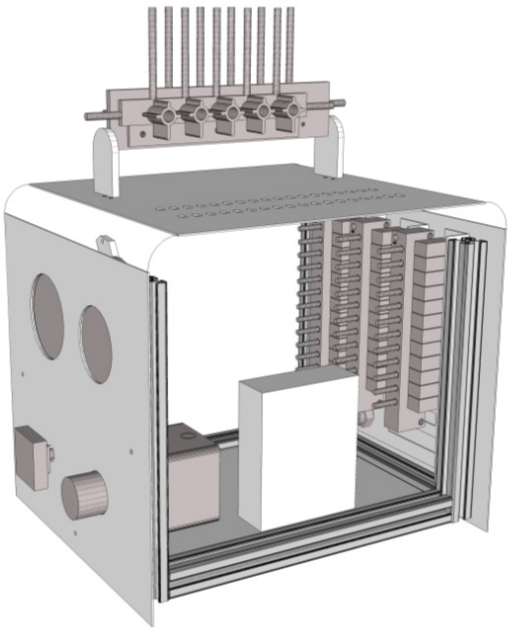

3D CAD of the Microfluidics module.

- Sensor and electronic control Box:

The main advantage of this box is the possibility to extract the optical sensor in order to align and then, as a robust system we can introduce into the box without moving any component.

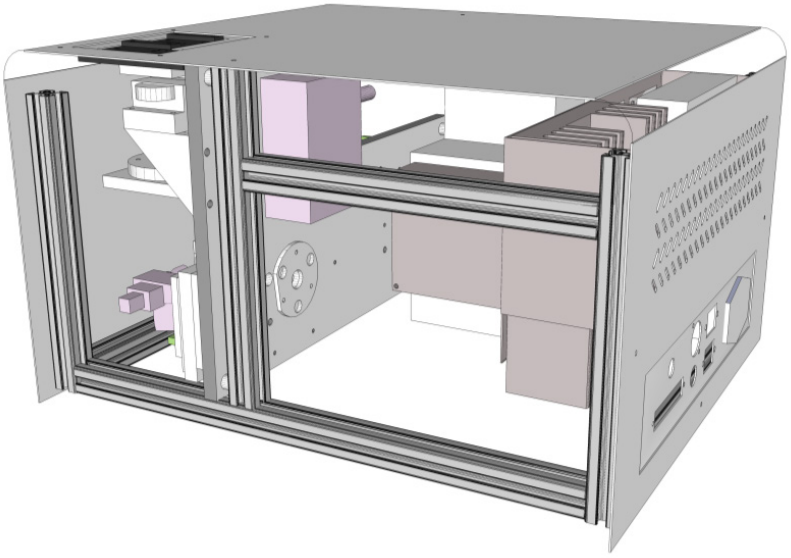

3D CAD of the Sensor (and electronic control) module.